Electronics and Communications in Japan, Vol. 92, No. 6, 2009
Translated from Denki Gakkai Ronbunshi, Vol. 128-C, No. 2, February 2008, pp. 286–294

Passivity-Based Control on Dynamic Visual Feedback Systems with Movable Camera Configuration

TOSHIYUKI MURAO,[1] HIROYUKI KAWAI,[2] and MASAYUKI FUJITA[3]
[1]Advanced Institute of Industrial Technology, Japan
[2]Kanazawa Institute of Technology, Japan
[3]Tokyo Institute of Technology, Japan

SUMMARY

This paper deals with control of dynamic visual feedback systems with a movable camera configuration. This configuration consists of a robot manipulator and a camera that is attached to the end-effector of another robot manipulator. This system, which can be interpreted as the dynamic visual feedback system with an eye-in-hand configuration and a fixed camera one as a special case, can enlarge the field of view. First, the dynamic visual feedback system with an eye-to-hand configuration is given with the fundamental representation of a relative rigid body motion. Second, we construct the dynamic visual feedback system with a movable camera configuration by combining the camera control error system. Next, we derive the passivity of the dynamic visual feedback system. Based on the passivity, stability and L_2-gain performance analysis are discussed. Finally the validity of the proposed control law can be confirmed by comparing the experimental results. © 2009 Wiley Periodicals, Inc. Electron Comm Jpn, 92(6): 1–11, 2009; Published online in Wiley InterScience (www.interscience.wiley.com). DOI 10.1002/ecj.10091

Key words: visual feedback control; manipulator dynamics; passivity; Lyapunov stability; L_2-gain performance analysis.

1. Introduction

Visual feedback control has been used for rather complicated systems in a wide application range, such as factory automation and medical treatment. In classical visual servoing, many practical methods are reported by two well-known approaches with two camera configurations, that is, position-based visual feedback control and image-based one with an eye-in-hand configuration or a fixed camera one [1, 2].

Recently, several camera configurations combining each classical one have been proposed to overcome the drawbacks which are that the eye-in-hand configuration cannot have global view whereas the fixed camera one is difficult to search throughout the workspace. Flandin and colleagues [3] addressed an eye-in-hand and a fixed camera cooperation approach where each camera information is partitioned into the positioning task and the orientation one, respectively. Elena and colleagues [4] proposed a method whereby the eye-in-hand camera executes the tracking of the target and the fixed one determines the position of the robot arm. In Ref. 5, the occlusion problem has been tackled by using multi eye-in-hand and fixed cameras.

On the other hand, instead of the use of additional cameras, an eye-to-hand configuration which has a movable camera installed at some place other than the work robot hand has also been proposed (including the fixed camera configuration as a particular case). Actually, such an eye-to-hand configuration using movable cameras allows effective visual servoing in complicated environments where repetitive operations are performed, such as welding or car coating [6]. There is also increasing demand for laparoscopic surgery manipulators and other medical robots; in addition to manipulator position and orientation control, such systems must provide for wide-area monitoring by a laparoscope or other device so as to maintain the field of view [7].

Sharma and Hutchinson [6] introduced the control method of a movable camera using motion perceptibility which relates magnitude of the rate of change in an object's position to that in the image of that object. Nelson and Khosla [8] described the movable camera control framework based on the camera's field of view and other indicators. Muis and Ohnishi [9] proposed a method to gain real-time visual servoing with a movable camera. However, these previous works [6, 8, 9] assume that the manipulator dynamics is negligible and does not interact with the visual feedback loop. Moreover, few results using movable cameras have been obtained for the stability of the closed-loop system and treated the tracking problem of moving target objects.

In this paper, we consider a dynamic visual feedback system using a movable camera as shown in Fig. 1. In particular, we analyze the stability and control performance of a system including one manipulator equipped with a camera (termed a camera manipulator), and another manipulator intended for actual operation (termed a work manipulator). The system proposed in this paper includes, as particular cases, the eye-in-hand configuration [10, 11] and the fixed camera configuration [12] proposed previously by the authors.

The paper is organized as follows. In Section 2 we explain a dynamic visual feedback system with the eye-to-hand configuration (including the fixed camera configuration). Section 3 presents a dynamic visual feedback system with the movable camera configuration combined with an error system for camera control. In addition, we propose a control law and perform an analysis of the stability and L_2-gain performance. We report experimental results obtained with a 2-DOF manipulator in Section 4, and give a summary in Section 5.

2. Dynamic Visual Feedback System with Eye-to-Hand Configuration

2.1 Representation of rigid motion in visual feedback system

In this paper, we consider a visual feedback system including two manipulators (a camera manipulator and a work one) using five coordinate frames as shown in Fig. 1. The five coordinate frames are: the world frame Σ_w based on the work manipulator, the hand frame Σ_h, the base frame of the camera manipulator Σ_z, the camera frame Σ_c, and the target object frame Σ_o. Throughout this paper, we use the notation $e^{\hat{\xi}\theta_{ij}} \in \mathcal{R}^{3\times3}$ to represent the rotation matrix of a frame Σ_j relative to a frame Σ_i. $\xi_{ij} \in \mathcal{R}^3$ specifies the direction of rotation and $\theta_{ij} \in \mathcal{R}$ is the angle of rotation. For simplicity we use $\hat{\xi}\theta_{ij}$ to denote $\hat{\xi}_{ij}\theta_{ij}$. The notation "$\wedge$" (wedge) is the skew-symmetric operator such that $\hat{a}b = a \times b$ for the vector cross-product $\times$ and any vector a, $b \in \mathcal{R}^3$, that is, $\hat{a}$ is a 3×3 skew-symmetric matrix. The notation "$\vee$" (vee) denotes the inverse operator to "$\wedge$," that is, $so(3) \to \mathcal{R}^3$. Recall that a skew-symmetric matrix corresponds to an axis of rotation (via the mapping $a \mapsto \hat{a}$). We use the 4×4 matrix

$$g_{ij} = \begin{bmatrix} e^{\hat{\xi}\theta_{ij}} & p_{ij} \\ 0 & 1 \end{bmatrix} \tag{1}$$

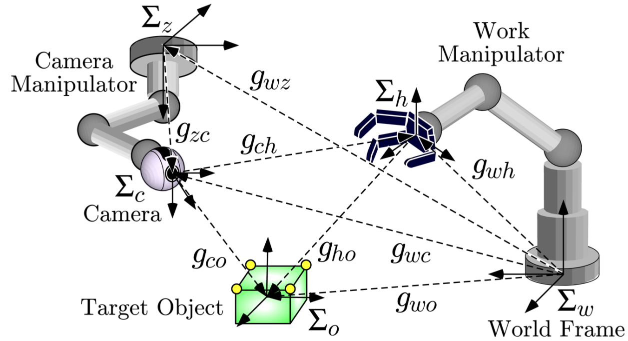

Fig. 1. Visual feedback system with movable camera configuration.

as the homogeneous representation of $g_{ij} = (p_{ij}, e^{\hat{\xi}\theta_{ij}}) \in SE(3)$ describing the configuration of a frame Σ_j relative to a frame Σ_i. For example, the position and orientation in the hand frame Σ_h relative to the world frame Σ_w is g_{wh}.

In our approach, g_{wh} and g_{zc} are obtained from the joint angle of each manipulator, and g_{wz} can be identified because the bases of the manipulators are fixed. In addition, g_{wc} and g_{ch} can be obtained from the composition rules for the homogeneous representation,* thus, the above position and orientation data are known. On the other hand, g_{wo}, g_{ho}, and g_{co} are unknown because the motion of the target object is unknown.

In this section, we consider a visual feedback system with the eye-to-hand configuration. The control objective is to always match the relative position and orientation g_{ho} of the target object, relative to the hand frame, to its reference g_{hd}. The relative position and orientation g_{ho} cannot be obtained directly. Thus, we consider first the motion of the target object g_{co} relative to the camera frame.

The relative position and orientation g_{co} of the target object, relative to the camera frame, can be expressed as follows:

$$g_{co} = g_{wc}^{-1} g_{wo} \tag{2}$$

In addition, the relative velocity of the target object, relative to the camera frame, can be obtained as the time derivative of Eq. (2):

$$V_{co}^b = -\mathrm{Ad}_{(g_{co}^{-1})} V_{wc}^b + V_{wo}^b \tag{3}$$

Here $V_{ij}^b \in \mathcal{R}^6$ is the body velocity of rigid motion, and $\mathrm{Ad}(g_{ij}) \in \mathcal{R}^6$ is the adjoint transformation of the homogeneous representation g_{ij} [13]. Equation (3) can be inter-

*From the relations between the three coordinate frames, $g_{wc} = g_{wz} g_{zc}$, $g_{ch} = g_{wc}^{-1} g_{wh}$.

preted as expressing the relative velocity V^b_{co} of the target object, relative to the camera frame, in terms of the difference between the camera velocity V^b_{wc} and the object velocity V^b_{wo}. Here $V^b_{wc} = 0$ corresponds to a fixed camera. For the detailed derivation, see Ref. 12.

2.2 Nonlinear observer and estimation error system

Here we consider the estimation error system. In this case, the image features are assumed to be acquired by means of a single pinhole camera. Although the visual information $f \in \mathcal{R}^{2m}$ obtained from the camera includes the relative position and orientation g_{co}, the latter cannot be obtained directly because the visual information is only two-dimensional.‡ Thus, a nonlinear observer is configured in order to obtain the estimated value $\bar{g}_{co}$ of the relative position and orientation. Based on Eq. (3), the motion model for the estimated value $\bar{g}_{co}$ is defined as follows:

$$\bar{V}^b_{co} = -\mathrm{Ad}_{(\bar{g}^{-1}_{co})} V^b_{wc} + u_e \tag{4}$$

Here $u_e \in \mathcal{R}^6$ is an additional input to stabilize the behavior of the estimation error. The design of the input u_e will be explained later.

The error g_{ee} between actual relative position and orientation and its estimate is defined as

$$g_{ee} := \bar{g}^{-1}_{co} g_{co} \tag{5}$$

In addition, the estimation error vector is defined as $e_e := [p^T_{ee} e^T_R(e^{\hat{\xi}\theta_{ee}})]^T \in \mathcal{R}^6$. Here $e_R(e^{\hat{\xi}\theta}) := \mathrm{sk}(e^{\hat{\xi}\theta})^{\vee} \in \mathcal{R}^3$, and $\mathrm{sk}(e^{\hat{\xi}\theta})^{\vee} := 1/2(e^{\hat{\xi}\theta} - e^{-\hat{\xi}\theta})$; $\mathrm{sk}(e^{\hat{\xi}\theta})$ is a function that extracts the skew-symmetric components of the rotation matrix. Using the visual information f acquired by the camera, the estimated visual information $\bar{f}$ obtained from the nonlinear observer, and the pseudo-inverse matrix $J^{\dagger}(\bar{g}_{co}) \in \mathcal{R}^{6\times 2m}$ of the image Jacobian, the estimation error vector e_e can be expressed as follows [12]:

$$e_e = J^{\dagger}(\bar{g}_{co})(f - \bar{f}) \tag{6}$$

If the estimation error vector e_e is zero, then the estimate of the relative position and orientation is equal to its actual value.

The estimation error system is configured using the basic representation of relative rigid body motion (3) and the nonlinear observer (4). In particular, by taking the time derivative of Eq. (5) and using Eqs. (3) and (4), the estimation error system is obtained as follows:

$$V^b_{ee} = -\mathrm{Ad}_{(g^{-1}_{ee})} u_e + V^b_{wo} \tag{7}$$

‡Details of the camera model are given in Ref. 12. Here the image features are acquired at $m(m \geq 4)$ feature points on the target object.

2.3 Hand control error system

In this subsection, let us consider the hand control error in order to achieve the control objective. The relative position and orientation g_{ho} of the target object relative to the hand frame cannot be obtained directly because g_{co} is not available. Thus, we consider the estimated value $\bar{g}_{ho}$*:

$$\bar{g}_{ho} = g^{-1}_{ch} \bar{g}_{co} \tag{8}$$

Differentiating Eq. (8) with respect to time, the estimated body velocity from Σ_h to Σ_o can be obtained as follows:

$$\bar{V}^b_{ho} = -\mathrm{Ad}_{(\bar{g}^{-1}_{ho})} V^b_{wh} + u_e \tag{9}$$

The hand control error g_{eh} can be defined as the difference between the estimated value $\bar{g}_{ho}$ of the relative position and orientation and the reference value g_{hd} of the target object relative to the hand frame:

$$g_{eh} := g^{-1}_{hd} \bar{g}_{ho} \tag{10}$$

In addition, similarly to the estimation error vector e_e, the hand control error vector is defined as $e_h := [p^T_{eh}\ e^T_R(e^{\hat{\xi}\theta_{eh}})]^T$.

Similarly to the estimation error system (7), the hand control error system can be obtained by taking the time derivative of Eq. (10):

$$V^b_{eh} = -\mathrm{Ad}_{(\bar{g}^{-1}_{ho})} V^b_{wh} + u_e - \mathrm{Ad}_{(g^{-1}_{eh})} V^b_{hd} \tag{11}$$

Here V^b_{hd} is the reference velocity of the target object g_{ho} relative to the hand frame.

2.4 Dynamic visual feedback system with eye-to-hand configuration

Here we configure a dynamic visual feedback system of the eye-to-hand configuration with the work manipulator's dynamics.

Assuming that the work manipulator has n_h degrees of freedom, its dynamics is expressed as follows [15]:

$$M_h(q_h)\ddot{q}_h + C_h(q_h, \dot{q}_h)\dot{q}_h + g_h(q_h) = \tau_h + \tau_{hd} \tag{12}$$

Here q_h, $\dot{q}_h$, $\ddot{q}_h \in \mathcal{R}^{n_h}$ are, respectively, the joint angle, angular velocity, and angular acceleration of the work manipulator, $\tau_h \in \mathcal{R}^{n_h}$ is the input torque, $\tau_{hd} \in \mathcal{R}^{n_h}$ is the disturbance input, $M_h(q_h) \in \mathcal{R}^{n_h \times n_h}$ is the inertia matrix, $C_h(q_h, \dot{q}_h)\, \dot{q}_h \in \mathcal{R}^{n_h}$ expresses the Coriolis and centrifugal forces, and $g_h(q_h) \in \mathcal{R}^{n_h}$ is the gravity force.

*We assume that the camera is calibrated properly, and that $g_{ch} = g^{-1}_{zc} g^{-1}_{wz} g_{wh}$ can be calculated accurately. In addition, the uncertainty of the external parameters can be reduced by the estimation for the robot hand aside from that for the target object [14].

In addition, the velocity of the robot hand can be expressed using the body manipulator Jacobian $J_{hb}(q_h) \in \mathcal{R}^{6\times n_h}$ as follows [13]:

$$V_{wh}^b = J_{hb}(q_h)\dot{q}_h \quad (13)$$

On the other hand, denoting the reference hand velocity by u_{hd} and the reference joint angular velocity by $\dot{q}_{hd}$, and using the body manipulator Jacobian just as in the above expression, $u_{hd} = J_{hb}(q_h)\dot{q}_{hd}$ can be written. The error of the joint angular velocity of the work manipulator is defined as $r_h := \dot{q}_h - \dot{q}_{hd} \in \mathcal{R}^{n_h}$. If this error r_h is zero, the hand velocity is equal to its reference value.

Now consider the following input torque applied to the work manipulator:

$$\begin{aligned}\tau_h = &M_h(q_h)\ddot{q}_{hd} + C_h(q_h, \dot{q}_h)\dot{q}_{hd} + g_h(q_h) \\ &+J_{hb}^T(q_h)\mathrm{Ad}_{(g_{hd}^{-1})}^T e_h + u_{rh}\end{aligned} \quad (14)$$

Here $\ddot{q}_{hd}$ is the reference value of the joint angular acceleration, and u_{rh} is an additional input to eliminate the error of the joint angular velocity; its setting will be explained later. Using Eqs. (7), (11), (12), and (14), the dynamic visual feedback system with the eye-to-hand configuration can be expressed as follows:

$$\begin{bmatrix} \dot{r}_h \\ V_{eh}^b \\ V_{ee}^b \end{bmatrix} = \begin{bmatrix} -M_h^{-1}C_h r_h + M_h^{-1}J_{hb}^T \mathrm{Ad}_{(g_{hd}^{-1})}^T e_h \\ -\mathrm{Ad}_{(\bar{g}_{ho}^{-1})} J_{hb} r_h \\ 0 \end{bmatrix} + \begin{bmatrix} M_h^{-1} & 0 & 0 \\ 0 & -\mathrm{Ad}_{(g_{eh}^{-1})} & I \\ 0 & 0 & -\mathrm{Ad}_{(g_{ee}^{-1})} \end{bmatrix} u_{fix} + \begin{bmatrix} M_h^{-1} & 0 \\ 0 & 0 \\ 0 & I \end{bmatrix} \begin{bmatrix} \tau_{hd} \\ V_{wo}^b \end{bmatrix} \quad (15)$$

where

$$u_{fix} := \begin{bmatrix} u_{rh} \\ \mathrm{Ad}_{(g_{hd}^{-1})} u_{hd} + V_{hd}^b \\ u_e \end{bmatrix} \quad (16)$$

The control objective in the dynamic visual feedback system with the eye-to-hand configuration is to make the robot hand follow the moving object. This objective is achieved by maintaining zero states r_h, e_h, and e_e.

(Note) Here camera motion is not discussed in this section. When camera motion is ignored, the dynamic visual feedback system with the eye-to-hand configuration (15) can be regarded as the dynamic visual feedback system with the fixed camera configuration [12].

3. Dynamic Visual Feedback Control with Movable Camera Configuration

In the previous section, we considered dynamic visual feedback control with the eye-to-hand configuration. In this system, however, the camera velocity V_{wc}^b was not considered as an input, which means that the target object might escape from the field of view. For example, in Ref. 12 we considered the fixed camera configuration, constituting a particular case of the eye-to-hand scheme at $V_{wc}^b = 0$. Usually, the fixed camera configuration is exploited in order to provide a larger field of view than the eye-in-hand scheme; however, a much wider field of view is required when the target object moves greatly.

Thus, using the advantages of a movable camera, we define the camera velocity V_{wc}^b as a system input so as to keep the object within the field of view. As shown in Fig. 1, we consider control of a camera mounted on a manipulator hand. Also note that the results of comparative experimental verification of the movable camera configuration and the fixed camera configuration are given below in Section 4.

3.1 Camera control error system

The control objective in this paper is always to keep g_{ho} equal to g_{hd}, while maintaining the relative position and orientation g_{co} of the target object, relative to the camera frame, at its reference value g_{cd} so that the camera does not lose the target object. However, as explained above, g_{co} cannot be obtained directly; thus, we use its estimated value $\bar{g}_{co}$. Here we define the camera control error between the estimated value $\bar{g}_{co}$ and the reference of the relative rigid body motion g_{cd} as

$$g_{ec} := g_{cd}^{-1}\bar{g}_{co} \quad (17)$$

In addition, the camera control error vector is defined as $e_c := [p_{ec}^T e_R^T(e^{\hat{\xi}\theta_{ec}})]^T$.

Just as in the hand control error system (11), we derive the camera control error system by taking the time derivative of Eq. (17):

$$V_{ec}^b = -\mathrm{Ad}_{(\bar{g}_{co}^{-1})} V_{wc}^b + u_e - \mathrm{Ad}_{(g_{ec}^{-1})} V_{cd}^b \quad (18)$$

where V_{cd}^b is the desired body velocity of the relative rigid body motion g_{co}.

3.2 Dynamic visual feedback system with movable camera configuration

In this subsection, we consider the dynamics of the camera manipulator in the same way as that of the work manipulator. The dynamics of a camera manipulator with n_c degrees of freedom is expressed as follows:

$$M_c(q_c)\ddot{q}_c + C_c(q_c, \dot{q}_c)\dot{q}_c + g_c(q_c) = \tau_c + \tau_{cd} \quad (19)$$

It should be noted that all the symbols of the camera manipulator have the same meaning as for the work one in Eq. (12).

In addition, the velocity of the camera can be expressed using the body manipulator Jacobian $J_{cb}(q_c) \in \mathcal{R}^{6\times n_c}$ as follows:

$$V^b_{wc} = J_{cb}(q_c)\dot{q}_c \tag{20}$$

On the other hand, by denoting the reference camera velocity by u_{cd} and reference joint angular velocity by $\dot{q}_{cd}$, and using the body manipulator Jacobian just as in the above expression, $u_{cd} = J_{cb}(q_c)\dot{q}_{cd}$ is obtained. The error of the joint angular velocity of the camera manipulator is defined as $r_c := \dot{q}_c - \dot{q}_{cd} \in \mathcal{R}^{n_c}$. Now consider the following input torque applied to the camera manipulator:

$$\begin{aligned}\tau_c = M_c(q_c)\ddot{q}_{cd} + C_c(q_c, \dot{q}_c)\dot{q}_{cd} + g_c(q_c)\\ +J^T_{cb}(q_c)\mathrm{Ad}^T_{(g^{-1}_{cd})}e_c + u_{rc}\end{aligned} \tag{21}$$

where $\ddot{q}_{cd}$ is the reference value of the joint angular acceleration. Using Eqs. (15), (18), (19), and (21), the dynamic visual feedback system with the movable camera configuration can be expressed as follows:

$$\begin{aligned}\begin{bmatrix}\dot{r}_h\\ \dot{r}_c\\ V^b_{eh}\\ V^b_{ec}\\ V^b_{ee}\end{bmatrix} &= \begin{bmatrix}-M_h^{-1}C_h r_h + M_h^{-1}J^T_{hb}\mathrm{Ad}^T_{(g^{-1}_{hd})}e_h\\ -M_c^{-1}C_c r_c + M_c^{-1}J^T_{cb}\mathrm{Ad}^T_{(g^{-1}_{cd})}e_c\\ -\mathrm{Ad}_{(\bar{g}^{-1}_{ho})}J_{hb}r_h\\ -\mathrm{Ad}_{(\bar{g}^{-1}_{co})}J_{cb}r_c\\ 0\end{bmatrix}\\ &+\begin{bmatrix}M_h^{-1} & 0 & 0 & 0 & 0\\ 0 & M_c^{-1} & 0 & 0 & 0\\ 0 & 0 & -\mathrm{Ad}_{(g^{-1}_{eh})} & 0 & I\\ 0 & 0 & 0 & -\mathrm{Ad}_{(g^{-1}_{ec})} & I\\ 0 & 0 & 0 & 0 & -\mathrm{Ad}_{(g^{-1}_{ee})}\end{bmatrix}u\\ &+\begin{bmatrix}M_h^{-1} & 0 & 0\\ 0 & M_c^{-1} & 0\\ 0 & 0 & 0\\ 0 & 0 & I\\ 0 & 0 & 0\end{bmatrix}w\end{aligned} \tag{22}$$

where

$$u := \begin{bmatrix}u_{rh}\\ u_{rc}\\ \mathrm{Ad}_{(g^{-1}_{hd})}u_{hd} + V^b_{hd}\\ \mathrm{Ad}_{(g^{-1}_{cd})}u_{cd} + V^b_{cd}\\ u_e\end{bmatrix},\ w := \begin{bmatrix}\tau_{hd}\\ \tau_{cd}\\ V^b_{wo}\end{bmatrix} \tag{23}$$

The control objective in the dynamic visual feedback system with the movable camera configuration is always to maintain the relative position and orientation of the target object from the viewpoints of the camera and hand at their respective references. This objective is achieved when the state $x := [r_h^T\ r_c^T\ e_h^T\ e_c^T\ e_e^T]^T$ is kept at zero.

The movable camera configuration makes possible a wider field of view than the fixed one, which offers a larger robot workspace. In the previous work [12], the workspace cannot be expanded unless the camera is fixed at a position providing a wide field of view. On the other hand, in the system proposed in this paper, the camera can track the target object at a short distance, and hence there is no need for a wide view angle. As a result, the extraction of unnecessary features other than the target object can be avoided. In addition, the visual feedback system with the movable camera configuration without regard for manipulator dynamics can be developed by using only Eqs. (7), (11), and (18), which is suitable for such applications as mobile robots. A block diagram of the dynamic visual feedback system with the movable camera configuration is shown in Fig. 2.

3.3 Passivity of dynamic visual feedback system

Here we derive the properties of the dynamic visual feedback system with the movable camera configuration in order to propose a control law.

[Lemma 1] If $w = 0$, then the dynamic visual feedback system (22) satisfies

$$\int_0^T u^T \nu d\tau \geq -\beta_0,\ {}^\forall T > 0 \tag{24}$$

where ν is defined as

$$\begin{aligned}\nu &= Nx \\ N &:= \begin{bmatrix}I & 0 & 0 & 0 & 0\\ 0 & I & 0 & 0 & 0\\ 0 & 0 & -I & 0 & 0\\ 0 & 0 & 0 & -I & 0\\ 0 & 0 & \mathrm{Ad}_{(e^{-\hat{\xi}\theta_{eh}})} & \mathrm{Ad}_{(e^{-\hat{\xi}\theta_{ec}})} & -I\end{bmatrix}\end{aligned} \tag{25}$$

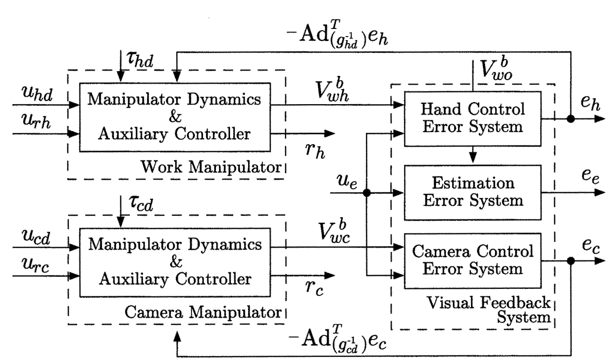

Fig. 2. Block diagram of dynamic visual feedback system with movable camera configuration.

and β_0 is a positive scalar.

(Proof) Consider the following energy function:

$$V = \frac{1}{2}r_h^T M_h r_h + \frac{1}{2}r_c^T M_c r_c + E(g_{eh}) + E(g_{ec}) + E(g_{ee}) \quad (26)$$

where $E(g_{ij}) := 1/2\|p_{ij}\|^2 + \phi(e^{\hat{\xi}\theta_{ij}})$ and $\phi(e^{\hat{\xi}\theta_{ij}}) := 1/2\mathrm{tr}(I - e^{\hat{\xi}\theta_{ij}})$ which is the error function of the rotation matrix [16]. Considering the skew-symmetry of the visual feedback system and the manipulator dynamics, the time derivative of the energy function V yields

$$\dot{V} = \frac{1}{2}r_h^T(\dot{M}_h - 2C_h)r_h + \frac{1}{2}r_c^T(\dot{M}_c - 2C_c)r_c + x^T N^T u = u^T \nu \quad (27)$$

Integration of both sides of the above expression gives

$$\int_0^T u^T \nu d\tau = V(T) - V(0) \geq -V(0) := -\beta_0 \quad (28)$$

where β_0 is a nonnegative constant that depends only on the initial state. □

The above lemma suggests that the dynamic visual feedback system (22) involves the passivity property. This dynamic visual feedback system with the movable camera configuration (22) can be treated as a dynamic visual feedback system with the eye-in-hand one so long as the work manipulator is ignored. That is, the dynamic visual feedback system with the eye-in-hand configuration presented in Refs. 10 and 11 is a particular case if the hand velocity is $V_{wh}^b = 0$, the reference value of the hand velocity is $u_{hd} = 0$, and the relative rigid body motion in the world coordinates is $g_{wz} = I$, while the hand control error e_h is ignored as well as the work manipulator. In addition, as explained in Section 2, the case of the dynamic visual feedback system with the fixed camera configuration [12] is also included. Therefore, the dynamic visual feedback system with the movable camera configuration (22) includes, as particular cases, the two generally known dynamic visual feedback systems with the eye-in-hand configuration and with the fixed camera one.

3.4 Stability analysis for dynamic visual feedback system

We now propose the following control input for the interconnected system:

$$u = -K\nu = -KNx, \quad K := \mathrm{diag}\{K_{rh}, K_{rc}, K_h, K_c, K_e\} \quad (29)$$

where $K_{rh} := \mathrm{diag}\{k_{rh1}, \ldots, k_{rhn_h}\}$ and $K_{rc} := \mathrm{diag}\{k_{rc1}, \ldots, k_{rcn_c}\}$ denote the positive gain matrix for each joint axis of the work manipulator and camera one, respectively. $K_h := \mathrm{diag}\{k_{h1}, \ldots, k_{h6}\}$, $K_c := \mathrm{diag}\{k_{c1}, \ldots, k_{c6}\}$, and $K_e := \mathrm{diag}\{k_{e1}, \ldots, k_{e6}\}$ are the positive gain matrices of x, y, and z axes of the translation and the rotation for the hand control error, the camera control one, and the estimation one, respectively.

Considering the passivity of the dynamic visual feedback system shown in Lemma 1, the following theorem can be derived for stability.

[Theorem 1] If $w = 0$, then the equilibrium point $x = 0$ for the closed-loop system (22) and (29) is asymptotic stable.

(Proof) Treating energy function (26) as a Lyapunov function candidate, time integration along the trajectory of Eqs. (22) and (29) gives the following with regard to Eq. (27):

$$\dot{V} = u^T \nu = -x^T N^T K N x \quad (30)$$

Since the gains K_{rh}, K_{rc}, K_h, K_c, and K_e are positive definite, the matrix K is positive definite, the matrix N is nonsingular, and the system equilibrium point $x = 0$ is asymptotically stable. □

Thus, we have shown the stability via Lyapunov method for the dynamic visual feedback system with the movable camera configuration, which is composed of the work manipulator and the camera one. It is interesting to note that stability analysis is based on the passivity as described in Eq. (24).

3.5 L_2-gain performance analysis for dynamic visual feedback system

Based on the dissipative systems theory, we consider L_2-gain performance analysis for the dynamic visual feedback system (22) in one of the typical problems, that is, the disturbance attenuation problem.

In order to derive simple gain conditions, we redefine $K_c = k_c I$ and $K_e = k_e I$ where k_c and k_e are positive scalars. In addition, we set the following conditions using a positive scalar γ:

$$K_{rh} - \frac{1}{2\gamma^2}I - \frac{1}{2}I > 0 \quad (31)$$

$$K_{rc} - \frac{1}{2\gamma^2}I - \frac{1}{2}I > 0 \quad (32)$$

$$K_h - \frac{1}{2}I - \frac{(2k_c - 1)l}{2k_c - 1 - 2l}I > 0 \quad (33)$$

$$k_c - \frac{1}{2} - l > 0 \quad (34)$$

$$k_e - \frac{1}{2\gamma^2} - \frac{1}{2} > 0 \quad (35)$$

where

$$l = \frac{k_e(\gamma^2 + 1)}{\gamma^2(2k_e - 1) - 1} \quad (36)$$

The following theorem can be established for control performance analysis.

[Theorem 2] Given a positive scalar γ and consider the control input (29) with the gains K_{rh}, K_{rc}, K_h, k_c, and k_e such that the inequalities (31) to (35) are satisfied, then the closed-loop system (22) and (29) has L_2-gain $\leq \gamma$.

(Proof) Consider the energy function V defined in Eq. (26) as a storage function. Differentiating the positive definite function V along the trajectory of the closed-loop system and using the method of completing the squares yield

$$\begin{aligned}
&\dot{V} + \frac{1}{2}\|x\|^2 - \frac{\gamma^2}{2}\|w\|^2 \\
&= -\frac{\gamma^2}{2}\left\| w - \frac{1}{\gamma^2}\begin{bmatrix} I\,0\,0\,0 & 0 \\ 0\,I\,0\,0 & 0 \\ 0\,0\,0\,0 & \mathrm{Ad}_{(e^{-\hat{\xi}\theta_{ee}})} \end{bmatrix} x \right\|^2 \\
&\quad + \frac{1}{2\gamma^2}\left\| \begin{bmatrix} I\,0\,0\,0 & 0 \\ 0\,I\,0\,0 & 0 \\ 0\,0\,0\,0 & \mathrm{Ad}_{(e^{-\hat{\xi}\theta_{ee}})} \end{bmatrix} x \right\|^2 \\
&\quad + x^T N^T u + \frac{1}{2}\|x\|^2 \\
&\leq \frac{1}{2\gamma^2} W \|x\|^2 + x^T N^T u + \frac{1}{2}\|x\|^2
\end{aligned} \tag{37}$$

where $W := \mathrm{diag}\{I, I, 0, 0, I\}$. Substituting control law (29), we obtain

$$\begin{aligned}
&\dot{V} + \frac{1}{2}\|x\|^2 - \frac{\gamma^2}{2}\|w\|^2 \\
&\leq -x^T N^T K N x + \frac{1}{2\gamma^2} W \|x\|^2 + \frac{1}{2}\|x\|^2 \\
&= -x^T P x
\end{aligned} \tag{38}$$

where

$$P := N^T K N - \frac{1}{2\gamma^2} W - \frac{1}{2} I \tag{39}$$

Assuming that $P \geq 0$, integration of both sides gives

$$\begin{aligned}
\int_0^T (\gamma^2\|w\|^2 - \|x\|^2)d\tau &\geq 2V(T) - 2V(0) \\
&\geq -2V(0) := -\beta
\end{aligned} \tag{40}$$

Here β is a nonnegative constant that depends only on the initial state.

Now P can be transformed as follows:

$$P = \begin{bmatrix}
K_{rh} - \frac{1}{2\gamma^2}I - \frac{1}{2}I & 0 & 0 & 0 & 0 \\
0 & K_{rc} - \frac{1}{2\gamma^2}I - \frac{1}{2}I & 0 & 0 & 0 \\
0 & 0 & K_h + k_e I - \frac{1}{2}I & k_e \mathrm{Ad}_{(e^{\hat{\xi}\theta_{eh}})}\mathrm{Ad}_{(e^{-\hat{\xi}\theta_{ec}})} & -k_e \mathrm{Ad}_{(e^{\hat{\xi}\theta_{eh}})} \\
0 & 0 & k_e \mathrm{Ad}_{(e^{\hat{\xi}\theta_{ec}})}\mathrm{Ad}_{(e^{-\hat{\xi}\theta_{eh}})} & \left(k_c + k_e - \frac{1}{2}\right) I & -k_e \mathrm{Ad}_{(e^{\hat{\xi}\theta_{ec}})} \\
0 & 0 & -k_e \mathrm{Ad}_{(e^{-\hat{\xi}\theta_{eh}})} & -k_e \mathrm{Ad}_{(e^{-\hat{\xi}\theta_{ec}})} & \left(k_e - \frac{1}{2\gamma^2} - \frac{1}{2}\right) I
\end{bmatrix} \tag{41}$$

Therefore, from the Schur complement, the necessary condition $P \geq 0$ can be modified as the conditions (31) to (35) in Theorem 2.* □

In this control performance analysis, the motion of the target object is treated as a disturbance; the influence of the object's motion on the system is weaker with smaller γ. In H_∞-type control, we can consider some problems by establishing the adequate generalized plant. This paper has discussed L_2-gain performance analysis for the disturbance attenuation problem. The proposed strategy can be extended for the other type of generalized plants of the dynamic visual feedback systems.

4. Experimental Case Study

4.1 Experimental setup

The experimental results on a 2-DOF manipulator (SICE-DD arm [15]) are shown in order to understand our proposed method simply, though it is valid for 3D dynamic visual feedback systems.

The manipulators and the coordinate frames are shown in Fig. 3. Five coordinate frames are defined for the left manipulator (camera manipulator) equipped with the camera, and right manipulator (work manipulator). Both manipulators are composed of Link 1 (0.2 m) and Link 2 (0.3 m). The manipulators are controlled by a dSPACE DS1005 digital control board (Power PC 750, 480 MHz). The images are acquired by a Sony XC-HR57 CCD camera (60 fps), and imported by a PicPort-Stereo-H4D PCI-bus frame grabber board (60 fps). Image processing is performed by the HALCON software; in particular, four object points are calculated.

Because of space limitations, we omit discussion of the experiments without disturbances used to verify Theorem 1. We describe the experiments with a moving target object used to verify the L_2-gain performance for various γ. In addition, we compare the proposed method with the previous method of Ref. 12 (visual feedback control with the fixed camera configuration) in terms of field of view.

In the experiments, the target object moved in a straight line for 4 seconds, and then described a "figure 8" motion for 5.6 seconds, as shown in Fig. 4. The initial

*Since the condition (31) to (35) is equivalent $P > 0$ and we assume the worst disturbance, these are only sufficient conditions.

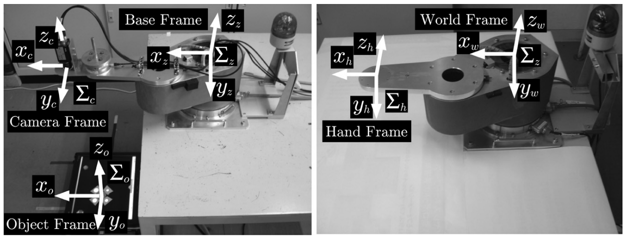

Fig. 3. Experimental arm (left: camera manipulator; right: work manipulator).

settings were: $p_{wh} = [0.4732\ 0.1\ 0]^T$, $\xi\theta_{wh} = [0\ 0\ 0]^T$, $p_{wz} = [0\ 0\ -1.16]^T$, $\xi\theta_{wz} = [0\ 0\ 0]^T$, $p_{wc} = [0.4732\ 0\ -1.16]^T$, $\xi\theta_{wc} = [0\ 0\ 0]^T$. In addition, we set the following time-invariant desired position and orientation: $p_{hd} = [0\ 0\ -2]^T$, $e^{\hat{\xi}\theta_{hd}} = I$, $p_{cd} = [0\ 0\ -0.84]^T$, $e^{\hat{\xi}\theta_{cd}} = I$. The error was assumed to be 0 at the initial state.

4.2 Experimental results for L_2-gain performance analysis

In the experiments, the gains were designed as follows, considering the disturbance attenuation problem.

Step 1: The gain K_h for the hand control error and the gain k_c for the camera control error are determined.

Step 2: The gain k_e for the estimation error is set so as to satisfy Eqs. (33) to (35).

Step 3: The gains K_{rh} and K_{rc} for the angular velocity errors are set so as to comply with the given γ and Eqs. (31) and (32).

Actually, the gains were set as follows.

Gain A: $\gamma = 0.388$, $k_c = 10$, $k_e = 20$, $K_h = \mathrm{diag}\{20, 20, 10, 10, 10, 20\}$, $K_{rh} = \mathrm{diag}\{5, 5\}$, $K_{rc} = \mathrm{diag}\{5, 5\}$

Gain B: $\gamma = 0.241$, $k_c = 30$, $k_e = 30$, $K_h = \mathrm{diag}\{50, 50, 25, 25, 25, 50\}$, $K_{rh} = \mathrm{diag}\{10, 10\}$, $K_{rc} = \mathrm{diag}\{10, 10\}$

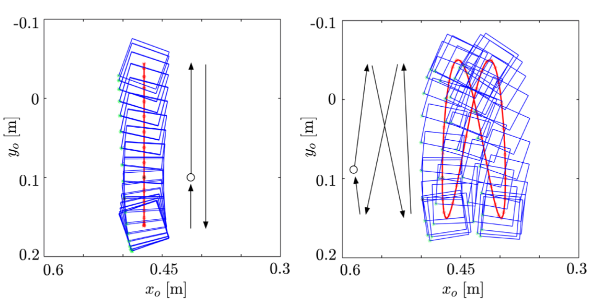

Fig. 4. Trajectory of target object.

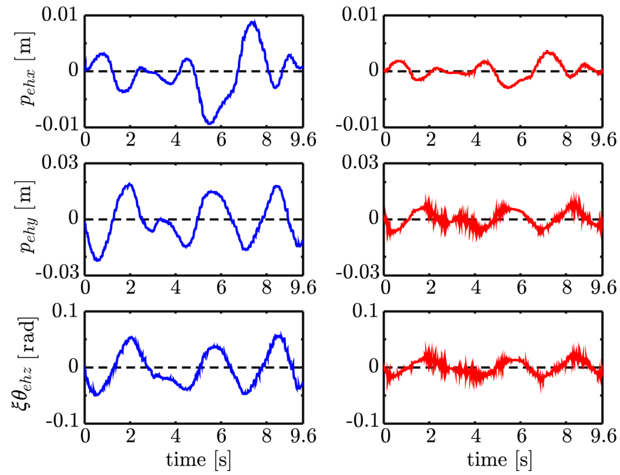

Fig. 5. Hand control error (left: Gain A; right: Gain B).

Comparative experimental results for the two gain settings are presented in Figs. 5 to 7. Figures 5 and 6 show the position errors of the x-axis and y-axis and the rotation error of the z-axis in 3D space. Figure 5 represents the hand control error, and Fig. 6 represents the camera control error. In addition, Fig. 7 shows the Euclidean norm $\|x\|$ of the state x. The left and right plots in Figs. 5 and 6, and the top and bottom plots in Fig. 7, represent Gain A and Gain B, respectively.

As indicated by the diagrams, Gain B with smaller γ exhibits smaller errors and better follow-up performance, which confirms the effectiveness of the proposed control law.

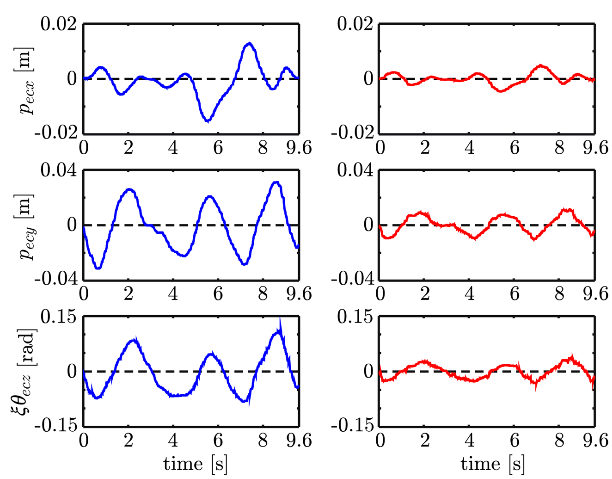

Fig. 6. Camera control error (left: Gain A; right: Gain B).

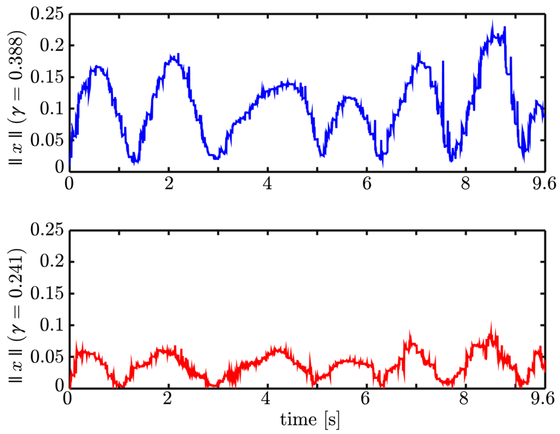

Fig. 7. State norm (top: Gain A; bottom: Gain B).

4.3 Experimental results for different camera configurations

We also compared the field of views obtained by the proposed movable camera configuration and by the previous fixed camera configuration. As explained in Section 3.3, the dynamic visual feedback system with the movable camera configuration proposed in this paper includes theoretically, as a particular case, the previously proposed dynamic visual feedback system with the fixed camera configuration. However, we have not yet considered the quantitative advantages of the movable camera configuration. Thus, we compared the two systems in terms of the field of view. In the experiments, we used Gain A and Gain B for the movable camera configuration, and k_e, K_h, and K_{rh} of Gain B for the fixed camera configuration.

Figure 8 shows the measured trajectories of four feature points of the target object: The left and right sides represent respectively the movable camera configuration with Gain B and the fixed camera configuration. (The case of the movable camera configuration with Gain A is omitted here because of space limitations.) The range of f_x and f_y shown in the diagrams corresponds to the actual measurement range provided by the camera in the experiments. Comparison between the two configurations indicates that the feature points of the moving target object approach the limits of the field of view in the case of a fixed camera, while staying in the middle area of the field of view in the case of a movable camera. This means that the movable camera tracks the target object properly.

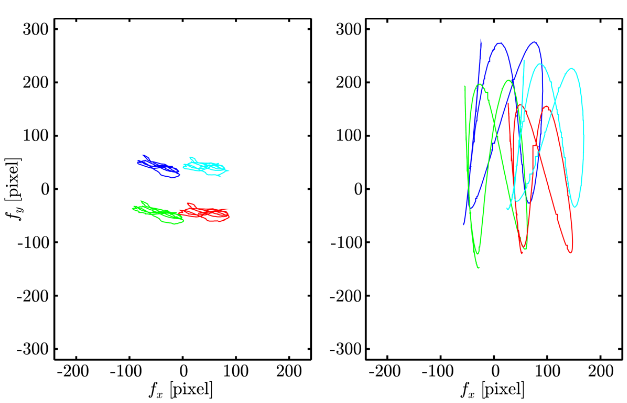

Fig. 8. Trajectory of feature points [left: movable camera (Gain B); right: fixed camera].

Moreover, Nelson and Khosla proposed the following index to evaluate the camera's field of view [17]:

$$fov = \frac{1}{\prod_{i=1}^{m}\left(1 - \frac{f_{xi}^2}{f_{xM}^2}\right)\left(1 - \frac{f_{yi}^2}{f_{yM}^2}\right)} \qquad (42)$$

Here $[f_{xi}\, f_{yi}]$ are the coordinates of the feature points on the image plane acquired by the camera, and $[f_{xM}\, f_{yM}]$ represent the respective maximum values. The closer the index is to 1 which represents the minimum value, the nearer the target object is to the image center. A high index means that the camera is located so that the target object is not likely to escape from the field of view.

Figure 9 shows how the field of view index varied with time in the experiments. The top and bottom diagrams represent respectively the fixed camera configuration and the movable camera configuration. The dashed and solid lines in the bottom diagram represent respectively Gain A and Gain B. From the diagrams, we can verify that the field of view index with the proposed control law is less than that with the previous one. This result states that the target object almost exists in the center of the camera, and the camera can move not to miss the moving target object. Thus, we may conclude that visual feedback control with the mov-

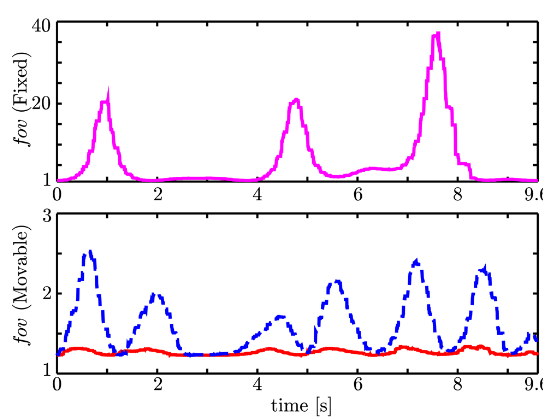

Fig. 9. Field of view index [top: fixed camera; bottom: movable camera (dashed line: Gain A; solid line: Gain B)].

able camera configuration offers a wider field of view than the fixed camera configuration.

5. Conclusions

In this paper, we considered a 3D dynamic visual feedback system with the movable camera configuration. Aiming at expansion of the robot's workspace, the proposed system which utilizes a movable camera includes, as particular cases, the eye-in-hand configuration and the fixed camera configuration. Stability and L_2-gain performance analysis for the dynamic visual feedback system have been discussed based on passivity with the energy function. We also carried out experiments to verify L_2-gain performance analysis and the effectiveness of the movable camera configuration.

REFERENCES

1. Hutchinson S, Hager GD, Corke PI. A tutorial on visual servo control. IEEE Trans Robotics Automation 1996;12:651–670.
2. Chaumette F, Hutchinson S. Visual servo control, Part I: Basic approaches. IEEE Robotics Automation Mag 2006;13:82–90.
3. Flandin G, Chaumette F, Marchand E. Eye-in-hand/eye-to-hand cooperation for visual servoing. Proc 2000 IEEE International Conference on Robotics and Automation, p 2741–2746.
4. Elena M, Cristiano M, Damiano F, Bonfe M. Variable structure PID controller for cooperative eye-in-hand/eye-to-hand visual servoing. Proc 2003 IEEE International Conference on Control Applications, p 989–994.
5. Lippiello V, Siciliano B, Villani L. Eye-in-hand/eye-to-hand multi-camera visual servoing. Proc 44th IEEE Conference on Decision and Control and European Control Conference, p 5354–5359, 2005.
6. Sharma R, Hutchinson S. Motion perceptibility and its application to active vision-based servo control. IEEE Trans Robotics Automation 1997;13:607–617.
7. Shimoyama I et al. Robot frontier. Iwanami Shoten; 2005. (in Japanese)
8. Nelson BJ, Khosla PK. Visually guided manipulation using active camera-lens systems. Proc 1997 IEEE International Conference on Robotics and Automation, p 437–442.
9. Muis A, Ohnishi K. Eye-to-hand approach on eye-in-hand configuration within real time visual servoing. IEEE/ASME Trans Mechatron 2005;10:404–410.
10. Kawai H, Azuma T, Fujita M. Observer-based dynamic visual feedback control of robotic systems. Trans Inst Syst Control Inf Eng 2004;17:39–47. (in Japanese)
11. Fujita M, Kawai H, Spong MW. Passivity-based dynamic visual feedback control for three dimensional target tracking-stability and L_2-gain performance analysis. IEEE Trans Control Syst Technol 2007;15:40–52.
12. Kawai H, Azuma T, Fujita M. Passivity-based 3D dynamic visual feedback control with a fixed camera. Trans Inst Syst Control Inf Eng 2005;18:127–135. (in Japanese)
13. Murray R, Li Z, Sastry SS. A mathematical introduction to robotic manipulation. CRC Press; 1994.
14. Kawai H, Murao T, Fujita M. Passivity-based dynamic visual feedback control with uncertainty of camera coordinate frame. Proc 2005 American Control Conference, p 3701–3706.
15. Kobayashi H et al. Practical control of robot manipulators. Corona; 1997. (in Japanese)
16. Bullo F, Lewis AD. Geometric control of mechanical systems. Springer-Verlag; 2004.
17. Nelson BJ, Khosla PK. Integrating sensor placement and visual tracking strategies. Proc 1994 IEEE International Conference on Robotics and Automation, p 1351–1356.

AUTHORS (from left to right)



Toshiyuki Murao received his B.E. degree from the Department of Electrical and Computer Engineering and M.E. degree from the Division of Electronics and Computer Science at Kanazawa University in 2003 and 2005, and D.Eng. degree from the Department of Mechanical and Control Engineering at Tokyo Institute of Technology in 2008. Since 2006, he has been an assistant professor at the Advanced Institute of Industrial Technology. His research focuses on the passivity-based visual feedback control of robot systems.

Hiroyuki Kawai received his B.S. degree from the Department of Electrical and Computer Engineering and M.S. and Ph.D. degrees from the Graduate School of Natural Science and Technology at Kanazawa University in 1999, 2001, and 2004. From 2004 to 2005, he was a postdoctoral scholar at the Information Technology Research Center, Hosei University. He has been an assistant professor at Kanazawa Institute of Technology since 2005. His research focuses on the visual feedback control of robot systems and the networked cellular vision system. In particular, he is interested in the passivity-based control. He received the IEEE Transactions on Control Systems Technology Outstanding Paper Award from the IEEE Control Systems Society (CSS) in 2008.

Masayuki Fujita received his B.E., M.E., and D.Eng. degrees in electrical engineering from Waseda University in 1982, 1984, and 1987. From 1985 to 1992, he was with the Department of Electrical and Computer Engineering at Kanazawa University. He was on the faculty of Japan Advanced Institute of Science and Technology as an associate professor from 1992 to 1998 and Kanazawa University as a professor in 1999. Since 2005, he has been a professor in the Department of Mechanical and Control Engineering, Tokyo Institute of Technology. From 1994 to 1995, he held a visiting position in the Department of Automatic Control Engineering, Technical University of Munich, Germany. His research interests include robust control and its applications, cooperative control, and passivity-based visual feedback. He will serve as the General Chair of the 2010 IEEE Multi-conference on Systems and Control. He currently serves as a member of the board of governors of the IEEE Control Systems Society, an Editor of the SICE Journal of Control, Measurement, and System Integration, and an Associate Editor of Automatica. He also served as a director of SICE in 2006 and Associate Editor of the IEEE Transactions on Automatic Control and Asian Journal of Control from 2005 to 2008. He received the 2008 IEEE Transactions on Control Systems Technology Outstanding Paper Award, the Best Paper Award from the Society of Instrument and Control Engineers in 1997, and from the Institute of Systems, Control and Information Engineers (ISCIE) in 2000.